SUPPLEMENTAL FIGURES

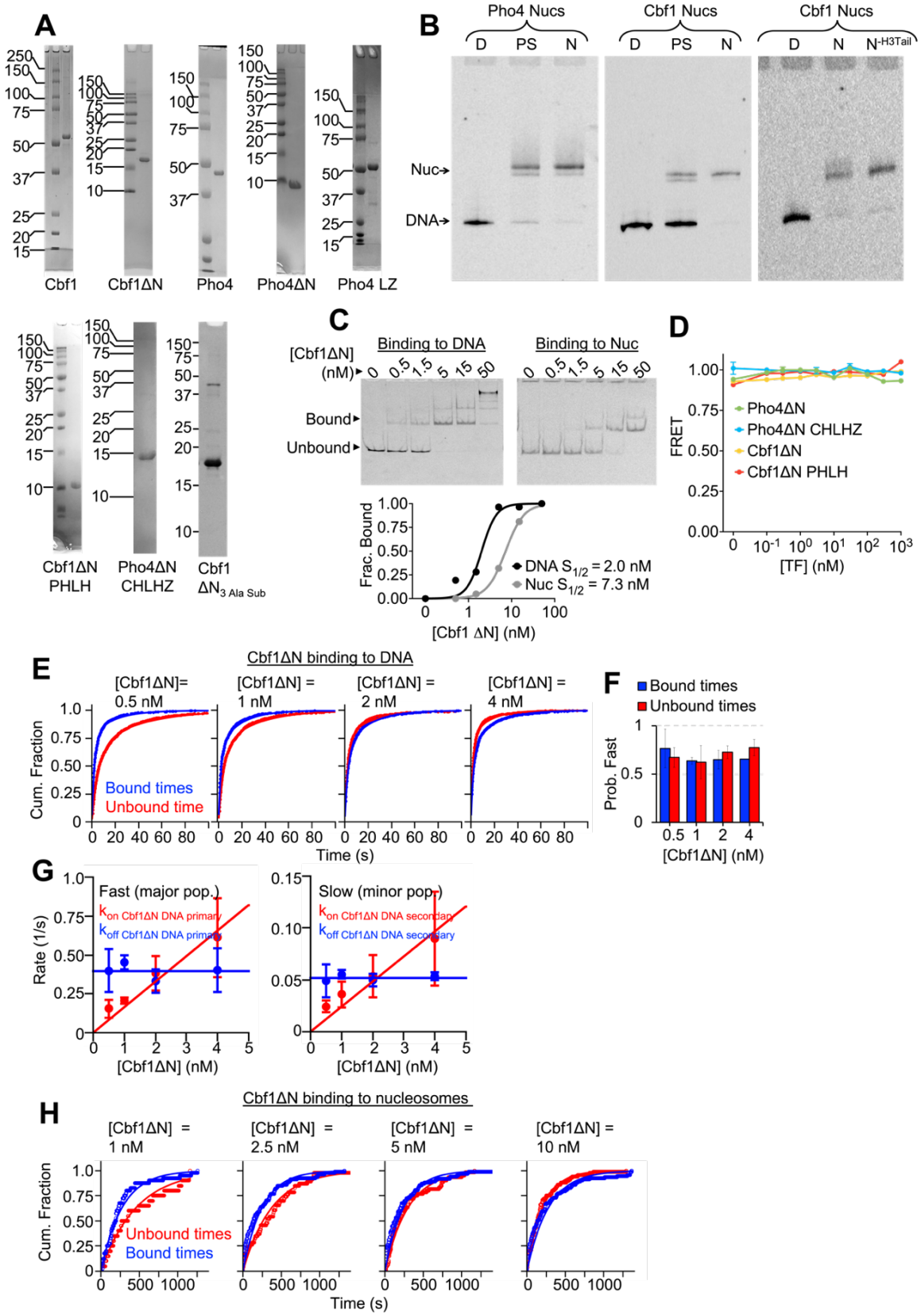

Figure S1. Protein/Nucleosome preparation and single-molecule characterization of Cbf1ΔN. Related to Figure 1. A) SDS gels of purified proteins used in this study. **B)** Representative native gels of nucleosomes used in this study, D = DNA, PS = pre-sucrose gradient purification, N = final nucleosomes. **C)** Electrophoresis mobility shift assays (EMSAs) to detect Cbf1ΔN binding to DNA (left) and nucleosomes (right). EMSAs are quantified below. **D)** Ensemble FRET assays where Pho4ΔN, Pho4ΔN CHLHZ, Cbf1ΔN, and Cbf1ΔN PHLH are titrated against 601 nucleosomes without a binding site. No change in FRET is detected indicating that the FRET decrease observed in nucleosome binding assays is due to specific binding. **E)** Cumulative sum distributions of bound (blue) and unbound dwell times (red) at all concentrations of Cbf1ΔN binding to DNA as measured through smPIFE. **F)** We determined that Cbf1ΔN binds DNA with two binding and two dissociation rates. Here, we illustrate the probability of bound (blue bars) or unbound (red bars) dwell times belonging to the fast population of events at each concentration of Cbf1ΔN. **G)** Primary (left) and secondary (right) binding and dissociation rates for Cbf1ΔN binding DNA. **H)** Cumulative sum distributions of bound (blue) and unbound dwell times (red) at all concentrations of Cbf1ΔN binding to nucleosomes as measured through smFRET. We determined that Cbf1ΔN binds nucleosomes with one binding and one dissociation rate.

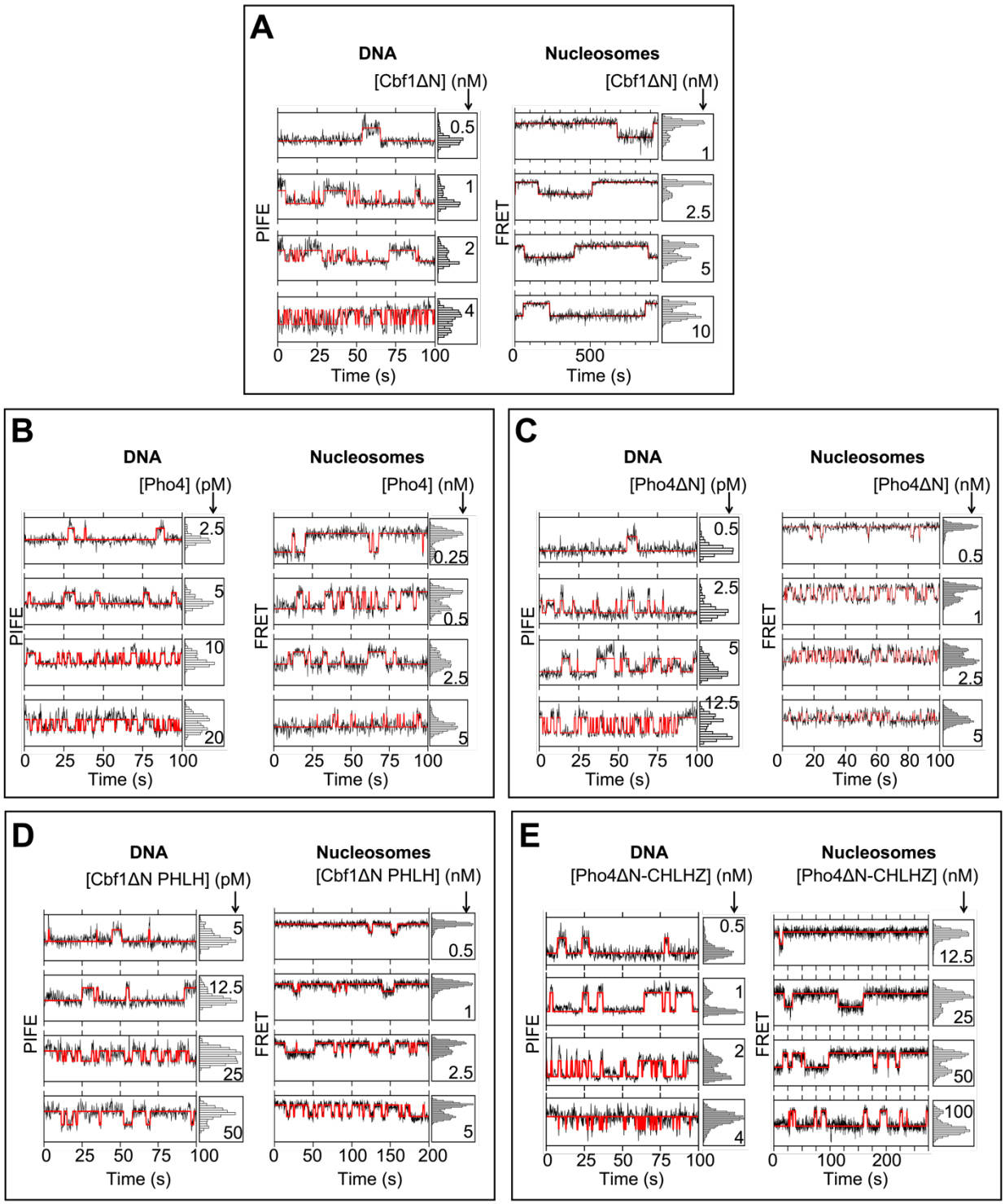

Figure S2. Representative example traces from smPIFE and smFRET measurements. **Related to Figures 1, 2, and 4.** Example time traces of (**A**) Cbf1ΔN, (**B**) Pho4, (**C**) Pho4ΔN, (**D**) Cbf1ΔN PHLH, and (**E**) Pho4ΔN CHLHZ binding to DNA and nucleosomes, respectively.

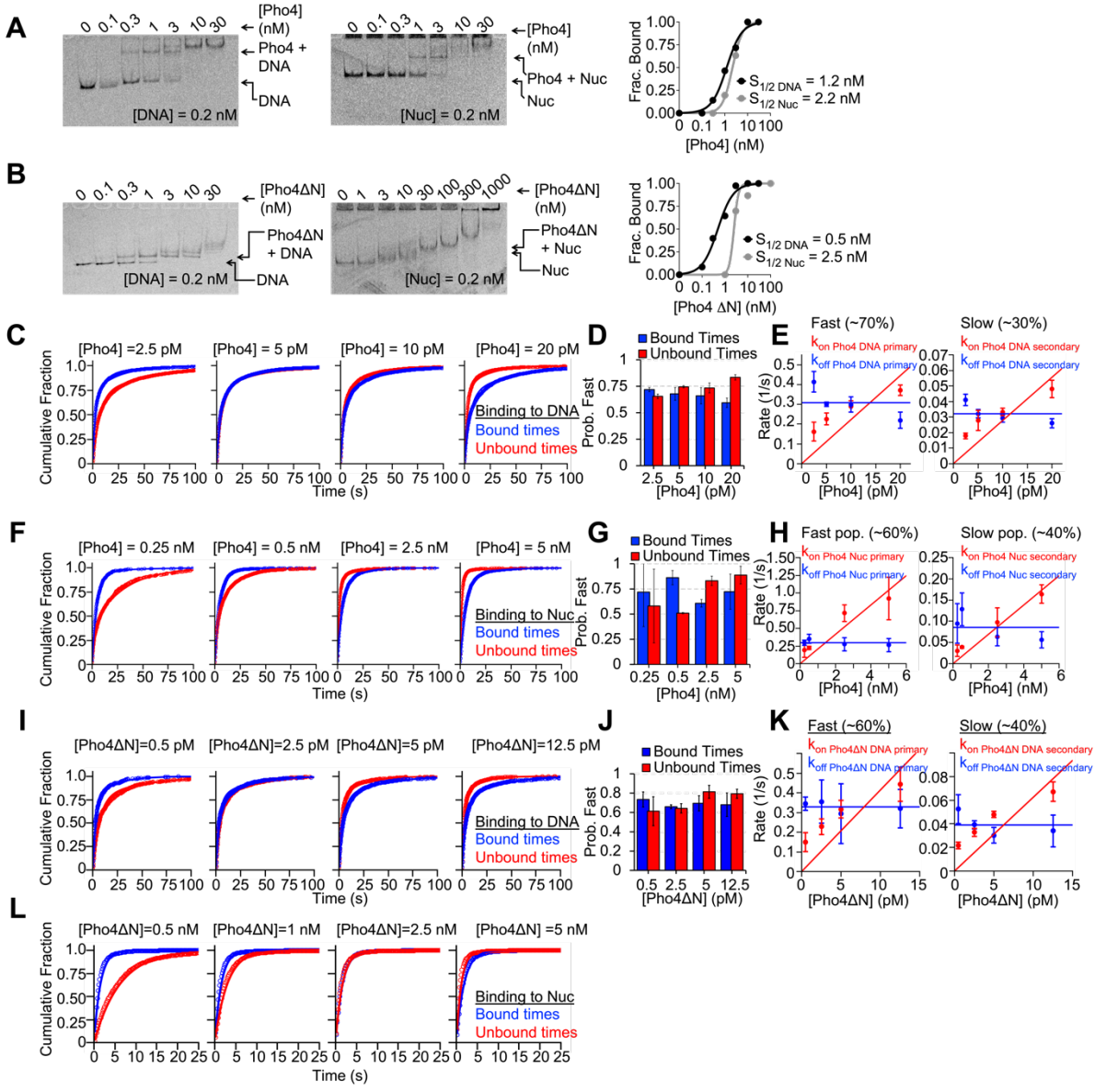
A
[Pho4] (nM)
Pho4 + DNA
DNA
[DNA] = 0.2 nM
[Nuc] = 0.2 nM
Pho4 + Nuc
Nuc
Frac. Bound
S1/2 DNA = 1.2 nM
S1/2 Nuc = 2.2 nM
[Pho4] (nM)
B
[Pho4ΔN] (nM)
Pho4ΔN + DNA
Pho4ΔN + Nuc
S1/2 DNA = 0.5 nM
S1/2 Nuc = 2.5 nM
[Pho4 ΔN] (nM)
C
[Pho4] =2.5 pM
[Pho4] = 5 pM
[Pho4] = 10 pM
[Pho4] = 20 pM
Cumulative Fraction
Binding to DNA
Bound times
Unbound times
Time (s)
D
Bound Times
Unbound Times
Prob. Fast
[Pho4] (pM)
E
Fast (~70%)
Slow (~30%)
kon Pho4 DNA primary
koff Pho4 DNA primary
kon Pho4 DNA secondary
koff Pho4 DNA secondary
Rate (1/s)
F
[Pho4] = 0.25 nM
[Pho4] = 0.5 nM
[Pho4] = 2.5 nM
[Pho4] = 5 nM
Binding to Nuc
G
H
Fast pop. (~60%)
Slow pop. (~40%)
kon Pho4 Nuc primary
koff Pho4 Nuc primary
kon Pho4 Nuc secondary
koff Pho4 Nuc secondary
I
[Pho4ΔN]=0.5 pM
[Pho4ΔN]=2.5 pM
[Pho4ΔN]=5 pM
[Pho4ΔN]=12.5 pM
J
K
Fast (~60%)
Slow (~40%)
kon Pho4ΔN DNA primary
koff Pho4ΔN DNA primary
kon Pho4ΔN DNA secondary
koff Pho4ΔN DNA secondary
L
[Pho4ΔN]=0.5 nM
[Pho4ΔN]=1 nM
[Pho4ΔN]=2.5 nM
[Pho4ΔN] =5 nM

Figure S3. Characterization of Pho4 and Pho4ΔN. Related to Figure 2. A) Characterization of Pho4 binding to DNA and nucleosomes by EMSA. Both gels are quantified on the right. **B**) Characterization of Pho4ΔN binding to DNA and nucleosomes by EMSA. Both gels are quantified on the right. **C)** Cumulative sum distributions of bound (blue) and unbound dwell times (red) at all concentrations of Pho4 binding to DNA as measured through smPIFE. **D)** We determined that Pho4 binds DNA with two binding and two dissociation rates. Here, we illustrate the probability of bound (blue bars) or unbound (red bars) dwell times belonging to the fast population of events at each concentration of Pho4. **E)** Primary (left) and secondary (right) binding and dissociation rates for Pho4 binding DNA at 4 concentrations. **F)** Cumulative sum distributions of bound (blue) and unbound dwell times (red) at all concentrations of Pho4 binding to nucleosomes as measured through smFRET. **G)** We determined that Pho4 binds nucleosomes with two binding and two dissociation rates. Here, we illustrate the probability of bound (blue bars) or unbound (red bars) dwell times belonging to the fast population of events at each concentration of Pho4. **H)** Primary (left) and secondary (right) binding and dissociation rates for Pho4 binding nucleosomes at 4 concentrations. **I)** Cumulative sum distributions of bound (blue) and unbound dwell times (red) at all concentrations of Pho4ΔN binding to DNA as measured through smPIFE. **J)** We determined that Pho4ΔN binds DNA with two binding and two dissociation rates. Here, we illustrate the probability of bound (blue bars) or unbound (red bars) dwell times belonging to the fast population of events at each concentration of Pho4ΔN. **K)** Primary (left) and secondary (right) binding and dissociation rates for Pho4ΔN binding DNA at 4 concentrations. **L)** Cumulative sum distributions of bound (blue) and unbound dwell times (red) at all concentrations of Pho4ΔN binding to nucleosomes as measured through smFRET. We determined that Pho4ΔN binds nucleosomes with one binding and one dissociation rate.

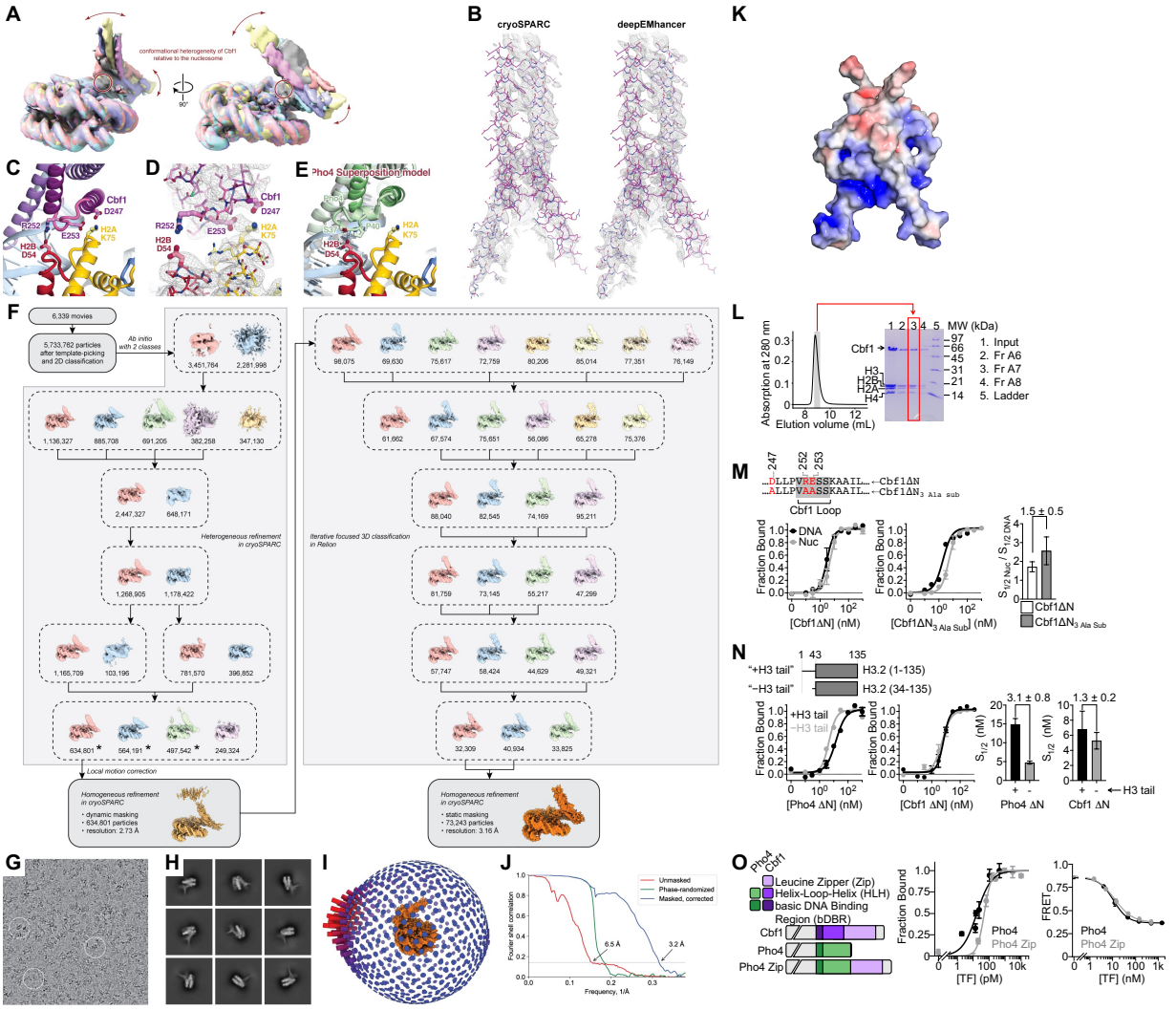

Figure S4. Cryo-EM analysis of Cbf1-nucleosome complex. Related to Figure 3. (A) Overlayed reconstructions of 3D classes illustrate the continuous movement of Cbf1 and the unwrapped DNA in multiple directions (red arrows). This movement pivots around the cluster of electrostatic interactions between Cbf1 and the histone core (red circle). The reconstructions were obtained by heterogeneous refinement of 1.7M particles into 6 classes in cryoSPARC, each color representing a distinct 3D class. **(B)** Cryo-EM map portion corresponding to Cbf1 dimer. On the left is the sharpened map from CryoSPARC Homogenous Refinement, and on the right, the same map after postprocessing with DeepEMhancer. The surface contour levels were set so that the encapsulated volume would be equal in both maps. **(C)** Electrostatic interactions in the Cbf1-histone interface: Cbf1(D247) on helix1 and Cbf1(E253) in the HLH loop both interact with H2A(K75), while Cbf1(R252) interacts with H2B(D54). **(D)** Similar view as **S4C** overlaid with map density. **(E)** Cbf1 has been replaced with superposed crystal structure model of Pho4 (PDB 1A0A). DNA and histones are from our Cbf1-nucleosome model. Pho4 residues that are within 5 Å of histones are highlighted. **(F)** Flowchart of 3D classification and reconstruction of the Cbf1-nucleosome complex dataset. The three classes marked with an asterisk (*) contain all 1.7M particles of the Cbf1-nucleosome complex. These were used to produce

the reconstructions in **panel A**. **(G)** Representative fragment of a micrograph. Particles used in the final reconstruction are circled. **(H)** Selected 2D class averages obtained from 2D classification of the particles used in the final reconstruction. **(I)** Euler angle distribution of the particles used in the final reconstruction. The view is the same as in **Figure 3A**. The length and color of the cylinders correspond to the number of particles assigned to an orientation. **(J)** FSC plots of final half maps refined independently in cryoSPARC. Resolution is determined at FSC = 0.143. In the phase-randomized FSC plot (green), phases were randomized beyond 6.5 Å. The FSC of masked half maps (blue) has been corrected using the phase-randomized FSC. **(K)** The APBS-calculated electrostatic potential for Pho4 mapped from -5 to 5 kT/e. **(L)** Size exclusion chromatogram of Cbf1-nucleosome complex reconstituted in 2:1 ratio (Cbf1 monomer:nucleosome). SDS-PAGE of the peak fraction (shaded area) displays histones H2A, H2B, H3 and H4, and Cbf1 in roughly stoichiometric amounts. We did not observe free nucleosome species in the eluate. The components of each fraction are shown in the SDS gel (right). **(M)** Left: binding curve for a new prep of Cbf1ΔN to DNA (black curve) and nucleosomes (grey curve). Middle: binding curve for $Cbf1\Delta N_{3\ Ala\ sub}$ to DNA (black curve) and nucleosomes (grey curve). Right: comparing nucleosome binding relative to DNA for Cbf1ΔN and $Cbf1\Delta N_{3\ Ala\ sub}$. We measure a 1.5 ± 0.5-fold decrease in binding affinity for the mutant. **(N)** Left: binding curve of Pho4ΔN to nucleosomes containing an H3 tail (black curve) or without an H3 tail (grey curve). Middle: binding curve of Cbf1ΔN binding to nucleosomes containing an H3 tail (black curve) or without an H3 tail (grey curve). Right: Removing H3 tail increases Pho4ΔN binding affinity by 3.1 ± 0.8-fold due to increased binding site accessibility. In contrast, removing H3 tail only increases Cbf1ΔN binding affinity by 1.3 ± 0.2-fold due to the contradictory effects of increased binding site accessibility and decreased interactions with the H3 tail. **(O)** Left: Domain diagrams of Cbf1, Pho4, and the Pho4 Zip chimera, in which the Cbf1 leucine zipper is inserted onto the C-terminus of Pho4. Middle: Ensemble PIFE measurements of Pho4 and Pho4 Zip binding at increasing concentrations to DNA. The x-axis displays the estimated concentration of unbound TF. In both experiments, we measure stoichiometric binding to DNA. Right: Ensemble FRET efficiency measurements of Pho4 and Pho4 Zip binding at increasing concentrations to nucleosomes. We measure no difference between Pho4 and Pho4 Zip binding affinity to nucleosomes: $S_{1/2\ Pho4\ Nuc}$ = 1.1 ± 0.1 nM, $S_{1/2\ Pho4\ Zip\ Nuc}$ = 1.2 ± 0.1 nM.

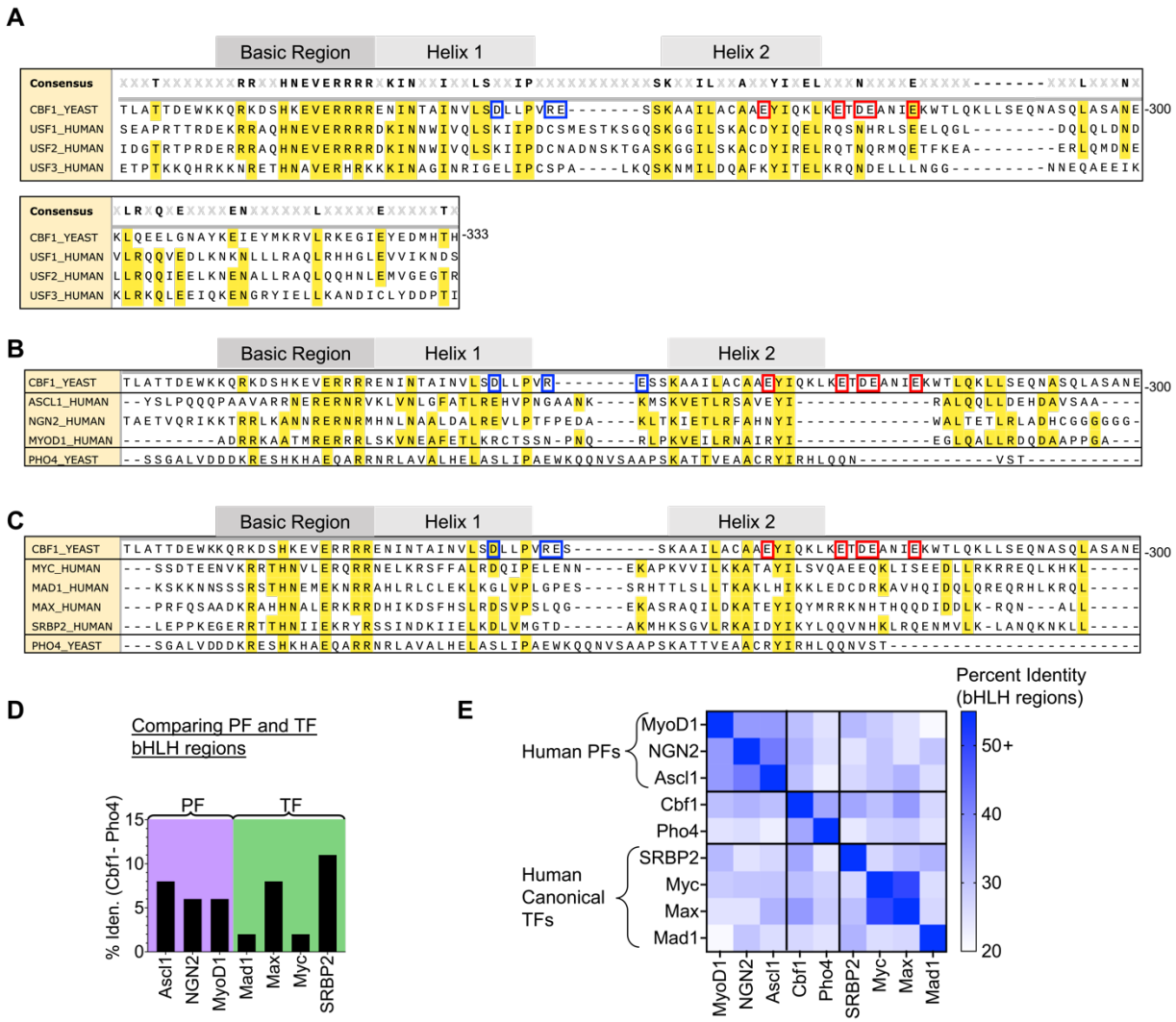

Figure S5. Aligning bHLH TFs and PFs. Related to Figure 3. (A) Alignment of Cbf1 bHLH region to USF1, USF2, and USF3. A consensus amino acid is assigned for positions that have greater than 50% agreement among the 4 proteins. Amino acids that agree with the consensus sequence are highlighted in yellow. Cbf1 D247, R252, E253, which directly contact histone octamer are indicated in blue boxes. Acidic solvent exposed residues positioned to interact with the H3 tail are indicated in red boxes. Alignment of Cbf1 and Pho4 to **(B)** known bHLH PFs Ascl1, Ngn2, and MyoD1 and **(C)** canonical TFs Myc, Mad1, Max, and SRBP2 in the same style as (A). **(D)** Comparing the difference in percent identity between Cbf1 and Pho4 to the known PFs and TFs. This analysis only considers bHLH regions. Both groups are more similar to Cbf1. **(E)** Percent identity matrix of the bHLH regions of Cbf1, Pho4, and the groups of PFs and TFs.

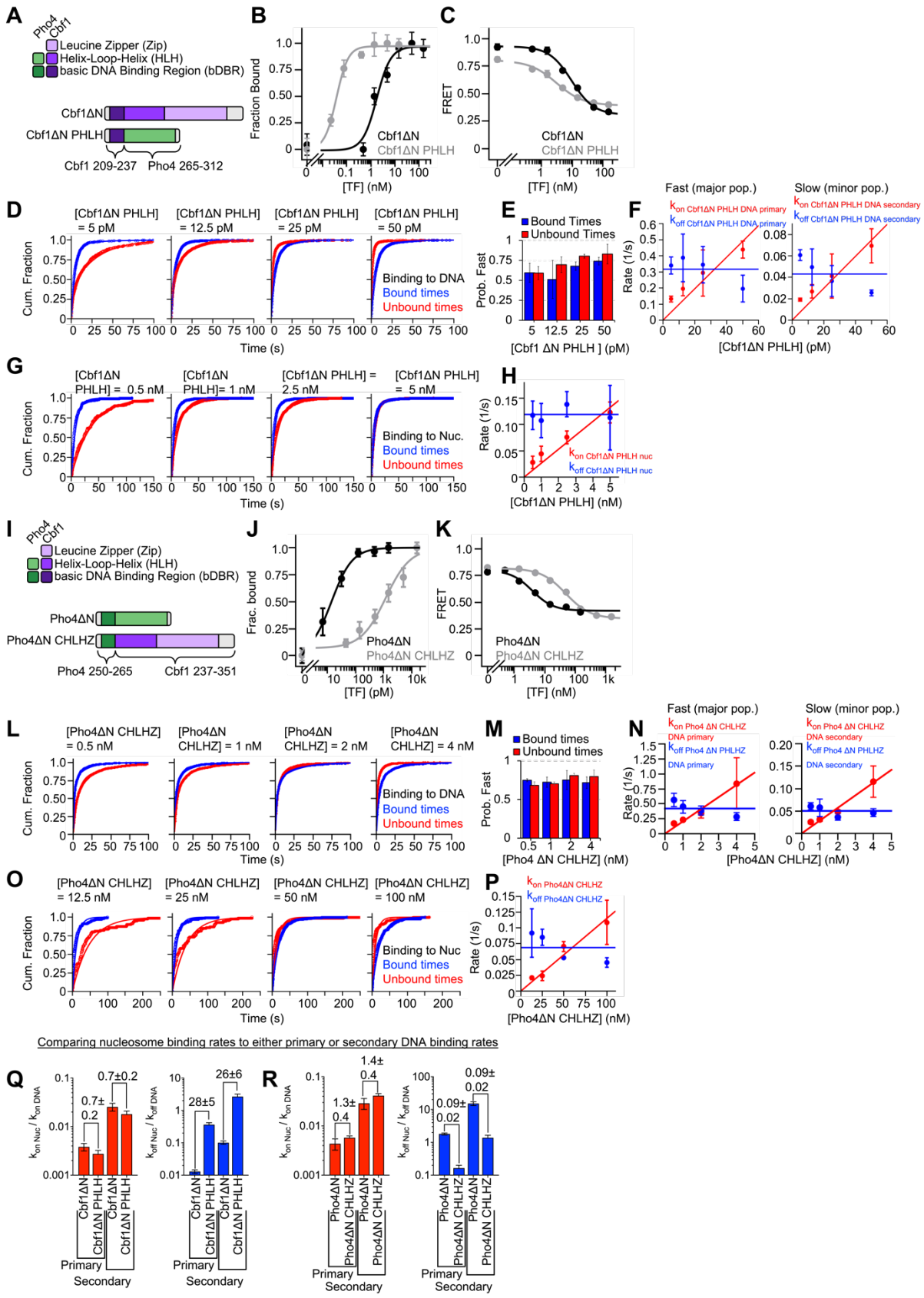
A
Pho4
Cbf1
Leucine Zipper (Zip)
Helix-Loop-Helix (HLH)
basic DNA Binding Region (bDBR)
Cbf1ΔN
Cbf1ΔN PHLH
Cbf1 209-237
Pho4 265-312
B
Fraction Bound
Cbf1ΔN
Cbf1ΔN PHLH
[TF] (nM)
C
FRET
Cbf1ΔN
Cbf1ΔN PHLH
[TF] (nM)
D
[Cbf1ΔN PHLH] = 5 pM
[Cbf1ΔN PHLH] = 12.5 pM
[Cbf1ΔN PHLH] = 25 pM
[Cbf1ΔN PHLH] = 50 pM
Cum. Fraction
Binding to DNA
Bound times
Unbound times
Time (s)
E
Bound Times
Unbound Times
Prob. Fast
[Cbf1 ΔN PHLH] (pM)
F
Fast (major pop.)
Slow (minor pop.)
Rate (1/s)
[Cbf1ΔN PHLH] (pM)
G
[Cbf1ΔN PHLH] = 0.5 nM
[Cbf1ΔN PHLH]= 1 nM
[Cbf1ΔN PHLH] = 2.5 nM
[Cbf1ΔN PHLH] = 5 nM
Cum. Fraction
Binding to Nuc.
Bound times
Unbound times
Time (s)
H
Rate (1/s)
[Cbf1ΔN PHLH] (nM)
I
Pho4
Cbf1
Leucine Zipper (Zip)
Helix-Loop-Helix (HLH)
basic DNA Binding Region (bDBR)
Pho4ΔN
Pho4ΔN CHLHZ
Pho4 250-265
Cbf1 237-351
J
Frac. bound
Pho4ΔN
Pho4ΔN CHLHZ
[TF] (pM)
K
FRET
Pho4ΔN
Pho4ΔN CHLHZ
[TF] (nM)
L
[Pho4ΔN CHLHZ] = 0.5 nM
[Pho4ΔN CHLHZ] = 1 nM
[Pho4ΔN CHLHZ] = 2 nM
[Pho4ΔN CHLHZ] = 4 nM
Cum. Fraction
Binding to DNA
Bound times
Unbound times
Time (s)
M
Bound times
Unbound times
Prob. Fast
[Pho4 ΔN CHLHZ] (nM)
N
Fast (major pop.)
Slow (minor pop.)
Rate (1/s)
[Pho4ΔN CHLHZ] (nM)
O
[Pho4ΔN CHLHZ] = 12.5 nM
[Pho4ΔN CHLHZ] = 25 nM
[Pho4ΔN CHLHZ] = 50 nM
[Pho4ΔN CHLHZ] = 100 nM
Cum. Fraction
Binding to Nuc
Bound times
Unbound times
Time (s)
P
Rate (1/s)
[Pho4ΔN CHLHZ] (nM)
Comparing nucleosome binding rates to either primary or secondary DNA binding rates
Q
0.7±0.2
0.7± 0.2
28±5
26±6
Primary
Secondary
R
1.4± 0.4
1.3± 0.4
0.09± 0.02
0.09± 0.02
Primary
Secondary

Figure S6. Characterization of Cbf1ΔN PHLH and Pho4ΔN CHLHZ. Related to Figure 4. (**A**). Domain diagrams of Cbf1ΔN and Cbf1ΔN PHLH in which the Pho4 dimerization domain (Pho4 residues 265-312) is inserted after Cbf1 residues 209-237. **(B)** Ensemble PIFE measurements of Cbf1ΔN and Cbf1ΔN PHLH binding at increasing concentrations to DNA ($S_{1/2\ Cbf1\Delta N\ DNA}$ = 1.8 ± 0.6 nM, $S_{1/2\ Cbf1\Delta N\ PHLH\ DNA}$ = 37 ± 5 pM). The x-axis represents the estimated concentration of unbound protein. **(C)** FRET efficiency measurements of Cbf1ΔN and Cbf1ΔN PHLH binding at increasing concentrations to nucleosomes ($S_{1/2\ Cbf1\Delta N\ Nuc}$ = 9.3 ± 1.3 nM, $S_{1/2\ Cbf1\Delta N\ PHLH\ Nuc}$ = 3 ± 0.2 nM). **(D)** Cumulative sum distributions of bound (blue) and unbound dwell times (red) at all concentrations of Cbf1ΔN PHLH binding to DNA as measured through smPIFE. **(E)** We determined that Cbf1ΔN PHLH binds DNA with two binding and two dissociation rates. Here, we illustrate the probability of bound (blue bars) or unbound (red bars) dwell times belonging to the fast population of events at each concentration of Cbf1ΔN PHLH. **(F)** Primary (left) and secondary (right) binding and dissociation rates for Cbf1ΔN PHLH binding DNA at 4 concentrations. **(G)** Cumulative sum distributions of bound (blue) and unbound dwell times (red) at all concentrations of Cbf1ΔN PHLH binding to nucleosomes as measured through smFRET. We determined that Cbf1ΔN PHLH binds nucleosomes with one binding and one dissociation rate. **(H)** Binding and dissociation rates for Cbf1ΔN PHLH binding nucleosomes at 4 concentrations. **(I)** Domain diagrams of Pho4ΔN and Pho4ΔN CHLHZ in which the Cbf1 dimerization domain (Cbf1 residues 237-351) is inserted after Pho4 residues 250-265. **(J)** Ensemble PIFE measurements of Pho4ΔN and Pho4ΔN CHLHZ binding at increasing concentrations to DNA ($S_{1/2\ Pho4\Delta N\ DNA}$ = 14 ± 1 pM, $S_{1/2\ Pho4\Delta N\ CHLHZ\ DNA}$ = 1.2 ± 0.5 nM). The x-axis represents the estimated concentration of unbound protein. **(K)** Measuring binding to nucleosomes at increasing concentrations of Pho4ΔN and Pho4ΔN CHLHZ by the ensemble FRET assay ($S_{1/2\ Pho4\Delta N\ Nuc}$ = 3.9 ± 0.9 nM, $S_{1/2\ Pho4\Delta N\ CHLHZ\ Nuc}$ = 49 ± 6 nM). **(L)** Cumulative sum distributions of bound (blue) and unbound dwell times (red) at all concentrations of Pho4ΔN CHLHZ binding to DNA as measured through smPIFE. **(M)** We determined that Pho4ΔN CHLHZ binds DNA with two binding and two dissociation rates. Here, we illustrate the probability of bound (blue bars) or unbound (red bars) dwell times belonging to the fast population of events at each concentration of Pho4ΔN CHLHZ. **(N)** Primary (left) and secondary (right) binding and dissociation rates for Pho4ΔN CHLHZ binding DNA. **(O)** Cumulative sum distributions of bound (blue) and unbound dwell times (red) at all concentrations of Pho4ΔN CHLHZ binding to nucleosomes as measured through smFRET. We determined that Pho4ΔN CHLHZ binds nucleosomes with one binding and one dissociation rate. **(P)** Binding and dissociation rates for Pho4ΔN CHLHZ binding nucleosomes at 4 concentrations. **(Q)** Comparison of nucleosome binding rates (red) and dissociation rates (blue) relative to DNA for Cbf1ΔN and Cbf1ΔN PHLH for both primary ($k_{on\ nuc}$ / $k_{on\ DNA\ primary}$) and secondary ($k_{on\ nuc}$ / $k_{on\ DNA\ primary}$) DNA binding rates. **(R)** Similar to (O) except now comparing nucleosome binding rates (red) and dissociation rates (blue) relative to DNA for Pho4ΔN and Pho4ΔN CHLHZ.

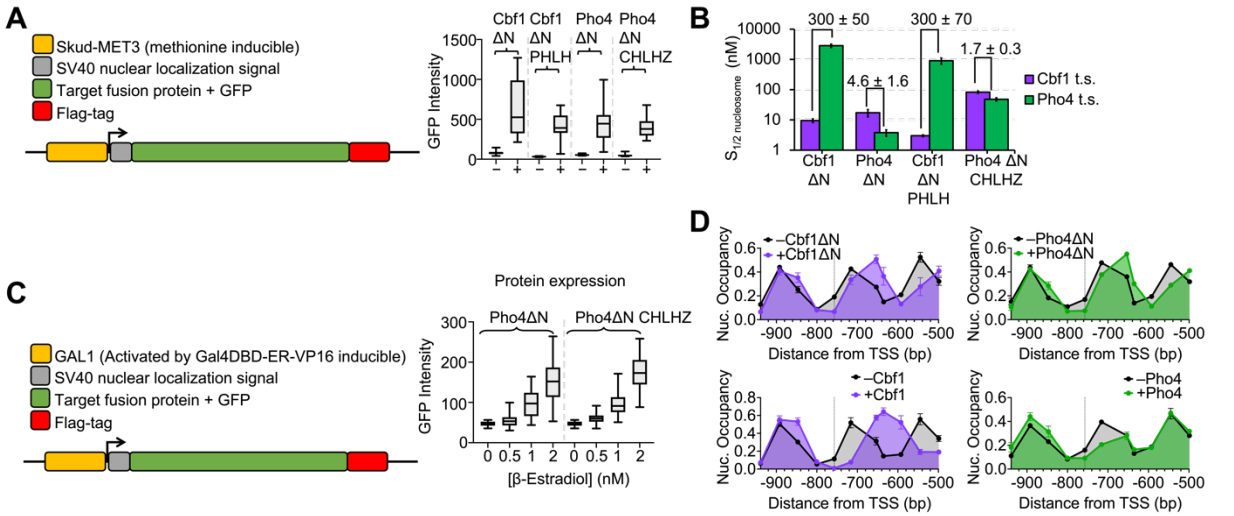

Figure S7. Establishing system for stable and inducible expression of protein constructs in live cells. Related to Figure 5. (A) Constructs for in vivo expression of Pho4-Cbf1 chimeras**.** GFP-tagged proteins are expressed from Met3 promoter in the absence of methionine. Protein expression is gauged by GFP intensity. Upon methionine depletion, all proteins are expressed to similar levels (right panel). (**B**) Ensemble FRET efficiency measurements of Cbf1ΔN, Cbf1ΔN PHLH, Pho4ΔN, and Pho4ΔN CHLHZ binding to the Cbf1 target site (t.s) (GGTCACGTGACC) and the Pho4 t.s. (CCCACGTGGG). $S_{1/2}$ for each titration was determined from fitting to a binding isotherm: Cbf1ΔN: $S_{1/2\ Cbf1\ b.s.}$ = 9.3 ± 1.3 nM, $S_{1/2\ Pho4\ b.s.}$ = 2800 ± 300 nM; Cbf1ΔN PHLH: $S_{1/2\ Cbf1\ b.s.}$= 3.0 ± 0.2 nM, $S_{1/2\ Pho4\ b.s.}$= 900 ± 210 nM; Pho4ΔN: $S_{1/2\ Cbf1\ b.s.}$= 17.3 ± 4.7 nM, $S_{1/2\ Pho4\ b.s.}$= 3.8 ± 0.9; Pho4ΔN CHLHZ: $S_{1/2\ Cbf1\ b.s.}$ = 83 ± 7 nM, $S_{1/2\ Pho4\ b.s.}$= 48 ± 6 nM. Bar graph represents $S_{1/2}$ values from the ensemble FRET measurements. Proteins containing the Pho4 basic region (Pho4ΔN and Pho4ΔN CHLHZ) bind similarly to both sites. Proteins containing the Cbf1 basic region (Cbf1ΔN and Cbf1ΔN PHLH) have a strong preference for the Cbf1 consensus site. (**C)** High regulation of protein expression levels was accomplished using a GAL1 promoter activated by GAL4DBD-ER-VP16. Titration of β-Estradiol shows concentration-dependent expression of GFP intensity and that both proteins are expressed to similar levels (right panel). For both plots, whiskers represent the complete range of GFP intensity values (minimum to maximum). **(D)** Comparison of nucleosome repositioning by full length vs ΔN Cbf1 and Pho4. Purple: Nucleosome occupancy within the *HO* promoter that contains a Cbf1 target site (indicated by grey dashed line) upon induction of either Cbf1ΔN (top) or full-length Cbf1 (bottom). Green: Nucleosome occupancy within the *HO* promoter that contains a Pho4 target site upon induction of either Pho4ΔN (top) or full-length Pho4 (bottom).

SUPPLEMENTAL TABLES

TF	$S_{1/2\ DNA}$ (nM)	$S_{1/2\ Nuc}$ (nM)	$S_{1/2\ Nuc}$ / $S_{1/2\ DNA}$
Cbf1 WT	0.5 ± 0.1	5.9 ± 0.8	12 ± 3
Cbf1ΔN	2.4 ± 0.5	7.2 ± 1.0	3.0 ± 0.7
Cbf1ΔN PHLH	0.037 ± 0.005	3.0 ± 0.2	80 ± 10
Pho4 WT	0.03 ± 0.02	1.08 ± 0.04	40 ± 30
Pho4ΔN	0.014 ± 0.001	3.9 ± 0.9	270 ± 70
Pho4ΔN CHLHZ	1.2 ± 0.5	49 ± 6	40 ± 20

Table S1. Summary of binding affinities determined by ensemble fluorescence measurements. Related to Figures 1, 2, and 4.

TF	Rate type	$k_{on\ DNA}$ (s^{-1} nM^{-1})	$k_{off\ DNA}$ (s^{-1})	K_D (nM)	Substrate
Cbf1 WT	Single	0.025 ± 0.006	0.30 ± 0.05	12.0 ± 3.5 nM	DNA
Cbf1ΔN	Primary	0.16 ± 0.01	0.39 ± 0.02	2.4 ± 0.2 nM	
	Secondary	0.024 ± 0.002	0.05 ± 0.002	2.1 ± 0.2 nM	
Cbf1ΔN PHLH	Primary	9.8 ± 1.3	0.32 ± 0.04	32 ± 6 pM	
	Secondary	1.5 ± 0.2	0.043 ± 0.008	29 ± 7 pM	
Pho4 WT	Primary	22 ± 5	0.31 ± 0.04	14 ± 3 pM	
	Secondary	2.8 ± 0.5	0.032 ± 0.003	11 ± 2 pM	
Pho4ΔN	Primary	40 ± 10	0.33 ± 0.01	8 ± 2 pM	
	Secondary	6.2 ± 1.4	0.039 ± 0.005	6.3 ± 1.6 pM	
Pho4ΔN CHLHZ	Primary	0.20 ± 0.01	0.42 ± 0.06	2.1 ± 0.3 nM	
	Secondary	0.028 ± 0.002	0.050 ± 0.005	1.8 ± 0.2 nM	
Cbf1 WT	Single	2.10E-04 ± 2.00E-05	1.11E-02 ± 7.00E-04	53 ± 6	Nucleosome
Cbf1ΔN	Single	6.12E-04 ± 1.00E-04	5.07E-03 ± 5.78E-04	8.3 ± 1.7	
Cbf1ΔN PHLH	Single	2.69E-02 ± 3.07E-03	1.15E-01 ± 8.27E-03	4.3 ± 0.6	
Pho4 WT	Primary	2.00E-01 ± 4.00E-02	3.00E-01 ± 2.00E-02	1.5 ± 0.3	
	Secondary	0.034 ± 0.004	0.09 ± 0.02	2.6 ± 0.7	
Pho4ΔN	Single	1.80E-01 ± 2.23E-02	5.93E-01 ± 3.23E-02	3.3 ± 0.4	
Pho4ΔN CHLHZ	Single	1.15E-03 ± 8.30E-05	6.88E-02 ± 1.16E-02	60 ± 11	

Table S2. Summary of primary and secondary binding and dissociation kinetics to and from DNA and nucleosomes. Related to Figures 1, 2, and 4.

TF	$k_{on\ Nuc}/\ k_{on\ DNA}$	$k_{off\ Nuc}/\ k_{off\ DNA}$	$K_{D\ Nuc}\ /\ K_{D\ DNA}$
Cbf1 WT	0.008 ± 0.002	0.037 ± 0.007	4.4 ± 1.4
Cbf1ΔN	0.0038 ± 0.0007	0.013 ± 0.002	3.4 ± 0.7
Cbf1ΔN PHLH	0.0027 ± 0.0005	0.36 ± 0.05	130 ± 30
Pho4 WT	0.009 ± 0.003	1.0 ± 0.1	110 ± 40
Pho4ΔN	0.004 ± 0.001	1.8 ± 0.1	400 ± 100
Pho4ΔN CHLHZ	0.0058 ± 0.0005	0.16 ± 0.04	29 ± 7

Table S3. Summary of nucleosome binding and dissociation kinetics relative to DNA. Related to Figures 1, 2, and 4.

Strain name	Genotype	Notes
yHC54-Cbf1dN	*can1, his3, leu2, trp1, ura2, hoprurs2 (nt-1298 to -272), ADE2, cbf1:GAL1pr-CBF1:TRP1, CLN2:HOpr-swi5mut-43Pho4-GFP:URA3, his3:SkudMET3pr-CBF1dN_GFP_3xFLAG:HIS3*	Cbf1 binding motif and Cbf1dN driven by Met promoter
yHC54-Cbf1dN_PDD	*can1, his3, leu2, trp1, ura2, hoprurs2 (nt-1298 to -272), ADE2, cbf1:GAL1pr-CBF1:TRP1, CLN2:HOpr-swi5mut-43Pho4-GFP:URA3, his3:SkudMET3pr-CBF1dN_PDD_GFP_3xFLAG:HIS3*	Cbf1 binding motif and Cbf1dN_PDD driven by Met promoter
yHC54-Pho4dN	*can1, his3, leu2, trp1, ura2, hoprurs2 (nt-1298 to -272), ADE2, cbf1:GAL1pr-CBF1:TRP1, CLN2:HOpr-swi5mut-43Pho4-GFP:URA3, his3:SkudMET3pr-PHO4dN_GFP_3xFLAG:HIS3*	Cbf1 binding motif and Pho4dN driven by Met promoter
yHC54-Pho4dN_CDD	*can1, his3, leu2, trp1, ura2, hoprurs2 (nt-1298 to -272), ADE2, cbf1:GAL1pr-CBF1:TRP1, CLN2:HOpr-swi5mut-43Pho4-GFP:URA3, his3:SkudMET3pr-PHO4dN_CDD_GFP_3xFLAG:HIS3*	Cbf1 binding motif and Pho4dN_CDD driven by Met promoter
yHC55-Cbf1dN	*can1, his3, leu2, trp1, ura2, hoprurs2 (nt-1298 to -272), ADE2, cbf1:GAL1pr-CBF1:TRP1, CLN2:HOpr-swi5mut-43Cbf1-GFP:URA3, his3:SkudMET3pr-CBF1dN_GFP_3xFLAG:HIS3*	Pho4 binding motif and Cbf1dN driven by Met promoter
yHC55-Cbf1dN_PDD	*can1, his3, leu2, trp1, ura2, hoprurs2 (nt-1298 to -272), ADE2, cbf1:GAL1pr-CBF1:TRP1, CLN2:HOpr-swi5mut-43Cbf1-GFP:URA3, his3:SkudMET3pr-CBF1dN_PDD_GFP_3xFLAG:HIS3*	Pho4 binding motif and Cbf1dN_PDD driven by Met promoter
yHC55-Pho4dN	*can1, his3, leu2, trp1, ura2, hoprurs2 (nt-1298 to -272), ADE2, cbf1:GAL1pr-CBF1:TRP1, CLN2:HOpr-swi5mut-43Cbf1-GFP:URA3, his3:SkudMET3pr-PHO4dN_GFP_3xFLAG:HIS3*	Pho4 binding motif and Pho4dN driven by Met promoter
yHC55-Pho4dN_CDD	*can1, his3, leu2, trp1, ura2, hoprurs2 (nt-1298 to -272), ADE2, cbf1:GAL1pr-CBF1:TRP1, CLN2:HOpr-swi5mut-43Cbf1-GFP:URA3, his3:SkudMET3pr-PHO4dN_CDD_GFP_3xFLAG:HIS3*	Pho4 binding motif and Pho4dN_CDD driven by Met promoter
yHC64-Pho4dN	*can1, his3, leu2, trp1, ura2, hoprurs2 (nt-1298 to -272), ADE2, cbf1:GAL1pr-CBF1:TRP1, CLN2:HOpr-swi5mut-43Pho4-GFP:URA3, his3:ADH1pr-GAL4DBD-ER-VP16::GAL1pr_-PHO4dN_GFP_3xFLAG:HIS3*	Pho4 binding motif and Pho4dN driven by GAL1 promoter
yHC64-Pho4dN_CDD	*can1, his3, leu2, trp1, ura2, hoprurs2 (nt-1298 to -272), ADE2, cbf1:GAL1pr-CBF1:TRP1, CLN2:HOpr-swi5mut-43Pho4-GFP:URA3, his3:ADH1pr-GAL4DBD-ER-VP16::GAL1pr-PHO4dN_CDD_GFP_3xFLAG:HIS3*	Pho4 binding motif and Pho4dN_CDD driven by GAL1 promoter

Table S4. Yeast strains used in this study. Related to Figure 5.

Cbf1 Nucleosome Primers	Binding motif: GGT**CACGTG**ACC
Cbf1 FRET fwd	Cy3-CTGGAGAGGT**CACGTG**ACCAGGCCGCTC
Rvs for FRET	biotin-CGCATGCTGCAGACGCGTT
Cbf1 DNA Primers	Binding motif: GGT**CACGTG**ACC
Cbf1 PIFE Fwd	Cy3-GGT**CACGTG**ACCTGCCGAGGCCGCTC
Rvs for PIFE	biotin-GCGGTTAAAAC[dT-Cy5]CGGGGGACAGCGC
Pho4 Nucleosome primers	Binding motif: CC**CACGTG**GG
Pho4 FRET fwd	Cy3-CTGGAGAACC**CACGTG**GGGAGGCCGCTCAATT
Rvs for FRET	biotin-CGCATGCTGCAGACGCGTT
Pho4 DNA primers	Binding motif: CC**CACGTG**GG
Pho4 PIFE fwd	Cy3-CC**CACGTG**GGCCGGTGCCGAGGCCGC
Rvs for PIFE	biotin-GCGGTTAAAAC[dT-Cy5]CGGGGGACAGCGC

Table S5. PCR primers for DNA used in single-molecule studies. Related to Figures 1, 2, and 4.

Statistics on PIFE experiments					
TF	Cbf1ΔN	Pho4	Pho4ΔN	Cbf1ΔN PHLH	Pho4ΔN CHLHZ
Total Molecules	9665	32735	8701	7720	10853
Fluc. w/ intensity	3383	4765	1323	1038	4341
Analyzed	541 (16% of 3383)	2428 (51% of 4765)	639 (48% of 1323)	519 (50% of 1038)	1005 (23% of 4341)
Acquisition rate	5 Hz	5 Hz	5 Hz	5 Hz	5 Hz
Statistics on FRET experiments					
TF	Cbf1ΔN	Pho4	Pho4ΔN	Cbf1ΔN PHLH	Pho4ΔN CHLHZ
Total Molecules	13204	10815	9486	8149	14703
FRET	2710	7553	3473	2385	3769
Analyzed	291 (11% of 2710)	1087 (14% of 7553)	780 (22% of 3473)	492 (21% of 2385)	442 (16% of 3769)
Acquisition rate	0.5 Hz	5 Hz	5 Hz	5 Hz	5 Hz

Table S6. Single molecule experiment statistics. Related to Figures 1, 2, and 4.

TF	Substrate		P-values for k_{on}				P-values for k_{off}			
Cbf1ΔN	DNA	[TF] (nM)	Trial 1	Trial 2	Trial 3		Trial 1	Trial 2	Trial 3	
		0.5	<1.00E-16	<1.00E-16	<1.00E-16		<1.00E-16	<1.00E-16	<1.00E-16	
		1	<1.00E-16	<1.00E-16	6.80E-08		<1.00E-16	<1.00E-16	<1.00E-16	
		2	<1.00E-16	<1.00E-16	<1.00E-16		<1.00E-16	5.00E-13	<1.00E-16	
		4	<1.00E-16	<1.00E-16	<1.00E-16		<1.00E-16	1.10E-16	7.70E-15	
Cbf1ΔN	Nuc	[TF] (nM)	Trial 1	Trial 2	Trial 3	Trial 4	Trial 1	Trial 2	Trial 3	Trial 4
		1	3.00E-04	2.00E-03	7.00E-01	4.00E-11	1.00E-03	1.00E-01	1.00E-02	3.00E-01
		2.5	1.00E-04	1.00E-01	4.00E-05	6.00E-02	2.00E-06	3.00E-08	1.00E-11	3.00E-02
		5	5.00E-02	6.00E-01	1.00E-03	5.00E-06	3.00E-08	3.00E-01	1.00E-06	1.00E-07
		10	9.00E-02	5.00E-01	1.00E+00	6.00E-01	9.00E-02	1.00E+00	6.00E-05	3.00E-02
Pho4	DNA	[TF] (pM)	Trial 1	Trial 2	Trial 3		Trial 1	Trial 2	Trial 3	
		2.5	<1.00E-16	<1.00E-16	<1.00E-16		<1.00E-16	<1.00E-16	<1.00E-16	
		5	<1.00E-16	<1.00E-16	<1.00E-16		<1.00E-16	<1.00E-16	<1.00E-16	
		10	<1.00E-16	<1.00E-16	<1.00E-16		<1.00E-16	<1.00E-16	<1.00E-16	
		20	<1.00E-16	<1.00E-16	<1.00E-16		<1.00E-16	<1.00E-16	<1.00E-16	
Pho4	Nuc	[TF] (nM)	Trial 1	Trial 2	Trial 3		Trial 1	Trial 2	Trial 3	
		0.25	1.30E-12	9.80E-11	<1.00E-16		2.20E-09	<1.00E-16	8.70E-09	
		0.5	<1.00E-16	<1.00E-16	<1.00E-16		<1.00E-16	<1.00E-16	2.60E-08	
		2.5	<1.00E-16	<1.00E-16	<1.00E-16		<1.00E-16	<1.00E-16	<1.00E-16	
		5	<1.00E-16	<1.00E-16	<1.00E-16		<1.00E-16	<1.00E-16	<1.00E-16	
Pho4ΔN	DNA	[TF] (pM)	Trial 1	Trial 2	Trial 3		Trial 1	Trial 2	Trial 3	
		0.5	<1.00E-16	<1.00E-16	5.00E-13		<1.00E-16	<1.00E-16	4.50E-09	
		2.5	<1.00E-16	<1.00E-16	<1.00E-16		<1.00E-16	<1.00E-16	<1.00E-16	
		5	<1.00E-16	<1.00E-16	<1.00E-16		<1.00E-16	<1.00E-16	<1.00E-16	
		12.5	<1.00E-16	<1.00E-16	<1.00E-16		<1.00E-16	<1.00E-16	<1.00E-16	
Pho4ΔN	Nuc	[TF] (nM)	Trial 1	Trial 2	Trial 3		Trial 1	Trial 2	Trial 3	
		0.5	1.00E-01	0.49	1		1.10E-05	9.90E-01	3.00E-02	
		1	1.90E-01	0.03	1		1.00E+00	4.10E-01	1.10E-09	
		2.5	6.60E-04	7.50E-07	3.70E-04		1.70E-02	2.20E-16	7.00E-01	
		5	2.70E-09	8.00E-06	2.30E-01		8.00E-05	5.10E-15	2.60E-05	
Cbf1ΔN PHLH	DNA	[TF] (pM)	Trial 1	Trial 2	Trial 3		Trial 1	Trial 2	Trial 3	
		5	<1.00E-16	<1.00E-16	3.30E-10		<1.00E-16	6.20E-08	3.20E-09	
		12.5	<1.00E-16	<1.00E-16	<1.00E-16		<1.00E-16	<1.00E-16	<1.00E-16	
		25	5.00E-13	<1.00E-16	<1.00E-16		<1.00E-16	<1.00E-16	<1.00E-16	
		50	<1.00E-16	<1.00E-16	2.80E-11		<1.00E-16	<1.00E-16	9.30E-11	
Cbf1ΔN PHLH	Nuc	[TF] (nM)	Trial 1	Trial 2	Trial 3		Trial 1	Trial 2	Trial 3	
		0.5	5.43E-01	5.10E-01	1.00E+00		6.00E-03	1.20E-02	8.20E-02	
		1	2.23E-01	3.00E-02	7.50E-01		1.00E+00	1.00E+00	1.00E-09	
		2.5	6.60E-05	9.00E-07			2.00E-02	2.20E-16		
		5	2.70E-09	1.30E-05	2.30E-01		7.00E-05	4.00E-15	2.40E-05	
Pho4ΔN CHLHZ	DNA	[TF] (nM)	Trial 1	Trial 2	Trial 3		Trial 1	Trial 2	Trial 3	
		0.5	<1.00E-16	<1.00E-16	<1.00E-16		<1.00E-16	<1.00E-16	<1.00E-16	
		1	<1.00E-16	<1.00E-16	<1.00E-16		<1.00E-16	<1.00E-16	<1.00E-16	
		2	<1.00E-16	<1.00E-16	<1.00E-16		<1.00E-16	<1.00E-16	<1.00E-16	
		4	<1.00E-16	<1.00E-16	<1.00E-16		<1.00E-16	5.90E-09	<1.00E-16	
Pho4ΔN CHLHZ	Nuc	[TF] (nM)	Trial 1	Trial 2	Trial 3		Trial 1	Trial 2	Trial 3	
		12.5	4.00E-04	2.00E-04	8.00E-01		2.00E-04	6.00E-01	2.00E-02	
		25	6.00E-07	1.00E-01	9.00E-02		3.00E-05	1.00E+00	7.00E-04	
		50	<1.00E-16	<1.00E-16			8.00E-14	1.00E-01		
		100	2.00E-12	<1.00E-16			6.00E-02	5.00E-04		

Table S7. P-values for the double exponential fits of cumulative probabilities of the unbound states. Related to Figures 1, 2, and 4.

Data collection and processing	
Microscope	Krios G3i #1 @ PNCC
Detector	K3 (Gatan)
Magnification	18,000x
Voltage (kV)	300
Electron exposure ($e^-/Å^2$)	50
Exposure time (s)	3.5
No. of frames	51
Dose rate ($e^-/Å^2$/frame)	0.98
Defocus range (μm)	-0.8 to -2.1
Pixel size (Å)	1.287 (0.644 super-res.)
Initial no. of particle images	1,696,534
Final no. of particle images	73,243
Map resolution (Å)	3.2
FSC threshold	0.143
Model validation	
MolProbity score	1.5
Clashscore	6.6
Rotamer outliers (%)	0.0
Ramachandran plot (%)	
Favored	97.4
Allowed	2.6
Outliers	0.0
B factors ($Å^2$)	
Protein	59
Nucleotide	72
Deposition	
PDB	7SSA
EMDB	EMD-25406
EMPIAR	EMPIAR-10875

Table S8. Cryo-EM data collection and refinement statistics. Related to Figure 3.

Primer name	sequence
P1-F-HO	CGATCCGTTTGGCGTCTT
P1-R-HO	TTCCTATTTGAGGTTGGTATTG
P2-F-HO	GGCGTTTGTGTATATTTTCATTC
P2-R-HO	GGGTATGAACCATACGATCAGT
P3-F-HO	CACAAACGCCACAATATACG
P3-R-HO	TGATCCGCTAATCagCGAC
P4-F-HO	CATACCCTGACTTGGCAAACC
P4.1-R-HO	CGCATTTTCGTGGATCCTC
P5.3-F-HO	GctGATTAGCGGATCACGAA
P5.3-R-HO	CACACGTCTACCATGTTGTCAG
P5.5-F-pCY12	GAGGATCCACGAAAATGcg
P5.4-R-pCY12	CGTGACGCACATGTCTgC
P6.51-F-HO	ATGGAAATTGATGCAGTTGcAG
P6.5-R-HO	CATGAATACATTTGCCCTTAAGCC
P7-F-pCY12	TGCAGTTGcAGACATGTGC
P7-R-HO	TAGTTACATCACTTTTCGTGACAC
P8-F-HO	CCTACACAGGGCTTAAGGG
P8-R-HO	TACACGCACAAAAAAGGTACG
P9-F-HO	GATGTAACTAAATACACGATTACC
P9-R-HO	GAAACAGGACTTGCGAACC
P10-F-HO	GTGCGTGTATTGAAATATTATGAC
P10-R-HO	CGTAAACCATAGGTTTATTTCG
PF1-EXO84	TCGCTAAACAAGATCACAGAA
PR1-EXO84	AGGAAATAGGTTAGTACACTGTCG

Table S9. MNase-qPCR primers used in this study. Related to Figure 5.

TF	Cbf1 binding site				Pho4 binding site			
	-757		-654		-757		-654	
	Occ. Ratio	*P*-value	Occ. Ratio	*P*-value	Occ. Ratio	*P*-value	Occ. Ratio	*P*-value
± Cbf1ΔN	0.35	0.008	1.85	0.008	0.77	0.436	1.31	0.030
± Pho4ΔN	0.96	0.755	0.97	0.572	0.44	1.45E-5	1.53	3.66E-5
± Cbf1ΔN PHLH	0.91	0.642	0.96	0.824	0.88	0.628	0.99	0.943
± Pho4ΔN CHLHZ	0.39	0.034	1.86	0.001	0.44	0.010	1.80	0.009

Table S10. The occupancy ratio and P-value for two genomic locations within nucleosome -4 with (+) and without (-) the indicated TF. The red numbers indicate changes that are statistically significant. Related to Figure 5.